EurJOC
European Journal of Organic Chemistry

Research Article
doi.org/10.1002/ejoc.202201209

Chemistry Europe
European Chemical Societies Publishing

www.eurjoc.org

Special Collection

Highly Conjugated Bis(benzo[*b*]phosphole)-*P*-oxides: Synthesis and Electrochemical, Optical, and Computational Studies

Nicolas D'Imperio,[a, b] Valentina Pelliccioli,[a] Sara Grecchi,[a] Alberto Bossi,[c, d] Francesca Vasile,[a] Silvia Cauteruccio,[a] Anna I. Arkhypchuk,[b] Arvind Kumar Gupta,[b] Andreas Orthaber,[b] Sascha Ott,*[b] and Emanuela Licandro*[a, d]

Dedicated to Professor Cesare Gennari on the occasion of his 70th birthday

The first examples of a π-conjugated benzo[*b*]phosphole *P*-oxide in which two phosphole *P*-oxide units are connected by a carbon-carbon double bond are described. The molecules are synthesized as *E* isomers with respect to the carbon-carbon double bond and exist as stable *cis* and *trans* isomers (chiral and meso one respectively) relatively to the two stereogenic P atoms. The optical and electrochemical properties of both isomers have been investigated by experiment and computations.

Introduction

Phosphole-based compounds with extended π-conjugation have been extensively studied as functional materials for organic electronic devices.[1] Phospholes are the phosphorus analogues of pyrroles and display unique electronic properties. While pyrrole is aromatic and has electron-donating character, phosphole has a lower aromaticity than furan and is therefore weakly aromatic, reflecting the low propensity of the phosphorus atom to delocalize its lone pair in the five-membered ring.[2] This intrinsic electronic structure confers to phospholes electron-accepting properties, which can be enhanced by means of different transformations involving the lone pair of the phosphorus atom. Such transformations include i) the coordination with transition metals,[3] ii) the formation of phosphonium salts,[4] and iii) the oxidation into phosphine oxides and phosphine sulphides.[3,5,6] The latter are the most useful systems for applications in organic electronics thanks to their thermal and chemical stability. In particular, benzo[*b*]phosphole *P*-oxides and their π-conjugated derivatives have attracted significant attention due to their intriguing luminescent properties (e.g., aggregation-induced emission, high quantum yields and photostability), that proved to be very useful for organic light-emitting diodes (OLEDs) technology,[7] photovoltaics,[8] and bioimaging.[9] Moreover, significant improvements have been made in the synthesis of phosphindole oxides and their modification through the introduction of different π-conjugated substituents onto the α and β positions of the phosphole ring.[10] Different synthetic methods towards π-conjugated benzo[*b*]phosphole *P*-oxides rely on the construction of the phosphole ring by multi-step sequences, including the intramolecular cyclization of 2-(arylethynyl)-phenylphosphine derivatives[11] or the intermolecular cycloaddition of internal arylacetylenes with phosphine derivatives,[12] in which the π-conjugated groups are incorporated into the starting materials. Otherwise, divergent syntheses of 2- or 3-aryl-, alkenyl- and alkynyl-benzo[*b*]phosphole derivatives have been developed using palladium chemistry (e.g. Stille, Suzuki, Heck, Sonogashira reactions) starting from 2-[13] or 3-[14] bromoareno[*b*]-phosphole *P*-oxides. Over the last years, some of us have been studying procedures to synthesize phosphole derivatives for potential applications in organic electronics.[15]

In our continued interest in the study of phosphole derivatives, we turned our attention to bis-(benzo[*b*]phosphole) *P*-oxides[9i,11f–h,13c] that are a subclass of phosphole *P*-oxides, in

[a] *Dr. N. D'Imperio, Dr. V. Pelliccioli, Dr. S. Grecchi, Prof. F. Vasile, Prof. S. Cauteruccio, Prof. E. Licandro*
Dipartimento di Chimica,
Università degli Studi di Milano
Via Golgi 19, 20133 Milano (Italy)
E-mail: emanuela.licandro@unimi.it
https://sites.unimi.it/licandrogroup/
[b] *Dr. N. D'Imperio, Dr. A. I. Arkhypchuk, Dr. A. Kumar Gupta, Prof. Dr. A. Orthaber, Prof. Dr. S. Ott*
Department of Chemistry, Ångström Laboratory,
Uppsala University
Box 523, 751 20 Uppsala (Sweden)
E-mail: sascha.ott@kemi.uu.se
https://www.kemi.uu.se/angstrom/research/synthetic-molecular-chemistry/research-groups/ott-group
[c] *Dr. A. Bossi*
Istituto di Scienze e Tecnologie Chimiche "Giulio Natta",
Consiglio Nazionale delle Ricerche (CNR-SCITEC)
Via Fantoli 16/15, 20138 Milano (Italy)
[d] *Dr. A. Bossi, Prof. E. Licandro*
SmartMatLab Center
via Golgi 19, 20133 Milano (Italy)

Supporting information for this article is available on the WWW under https://doi.org/10.1002/ejoc.202201209

Part of the "Cesare Gennari's 70th Birthday" Special Collection.

Research Article
doi.org/10.1002/ejoc.202201209

which the presence of two phosphindole oxide groups confers peculiar electronic and stereochemical features. Indeed, the introduction of two electron-withdrawing phosphole *P*-oxide moieties significantly increases the electron-accepting nature of these systems, while the presence of two stereogenic phosphorus atoms provides the *cis* and *trans* stereoisomers with respect to the directions of the P=O bonds. Some examples of both *cis* and *trans* bis-(benzo[*b*]phosphole) *P*-oxides have been reported in the literature and fully characterized (Figure 1, structure **A**, example of a *cis* isomer),[9i,11h,13c] whereas structures containing two phosphole *P*-oxide units connected by a π-spacer (i.e., phenyl ring) are still scarce, and attempts to separate the two diastereoisomers failed (Figure 1, structure **B**, example of a *cis* isomer).[11f,g,16]

Herein, we describe the study of an unexplored class of bis-(benzo[*b*]phosphole) *P*-oxides linked through a carbon-carbon double bond as π-spacer. The synthesis of the novel bis-benzo[*b*]phosphole *P*-oxide (*E*)-**1** has been investigated through transition metal-promoted coupling reactions starting from halogenated benzo[*b*]phospholes, including bromide **2a** and iodide **2b** (Figure 2), and the two *cis* and *trans* diastereoisomers of (*E*)-**1** have been analytically and spectroscopically characterized.

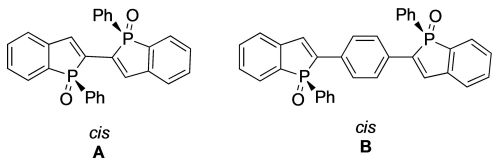

Figure 1. Structure of *cis* bis(benzo[*b*]phosphole) *P*-oxides.

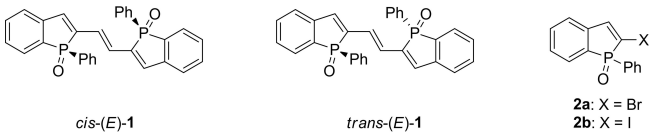

Figure 2. Structure of bis(benzo[*b*]phosphole) *P*-oxides *cis*-(*E*)-**1** and *trans*-(*E*)-**1**, and the benzo[*b*]phosphole halides **2a**,**b**.

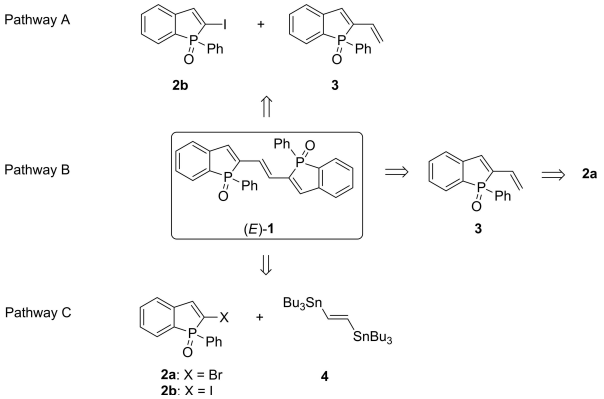

Scheme 1. Retrosynthetic analysis for the synthesis of olefin (*E*)-**1**.

The optical properties have been studied by absorption and emission spectroscopy (steady state and time resolved luminescence), and their electrochemical features have been determined by cyclic voltammetry. Preliminary DFT calculations have been performed as complementary characterization of these systems.

Results and Discussion

Strategies to synthesize olefin (*E*)-1

We envisaged a stereoselective synthesis of olefin (*E*)-**1** through the three different pathways A, B and C, starting from 2-halogenated benzophosphole *P*-oxide **2a** and **2b** (Scheme 1).

Pathways A and B are convergent syntheses and start from the common precursor 2-alkenylbenzo[*b*]phosphole *P*-oxide **3**, prepared by Stille coupling from bromide **2a** and the vinyl(tributyl)stannane.[13b] In Pathway A, the Heck cross-coupling reaction is utilized to combine alkene **3** with iodide **2b**, while in Pathway B olefin **1** can be obtained by the homometathesis reaction of **3**. The third, more straightforward alternative (Pathway C) to prepare **1** makes use of a double Stille coupling reaction between halides **2** and the commercially available *trans*-1,2-bis(tributylstannyl)ethene (**4**).

Synthesis of iodide 2b

Bromide **2a** was synthesized according to a literature procedure,[13c] while iodide **2b** is a novel compound. It could be prepared using an analogous method as that reported for the synthesis of **2a**. We first investigated the electrophilic iododesilylation of **5**[17] using *N*-iodosuccinimide (NIS, route *a)* Scheme 2). In particular, the reaction was performed using 3 equivalents of NIS in acetonitrile as solvent at 35 °C, and after 50 h the required iodide **2b** was isolated in 17% yield (Scheme 2).

Using iodine monochloride (ICl, route *b*) Scheme 2), as more reactive iodinating agent, we were able to obtain compound **2b** with a much better yield of 80%, and lower reaction time (4 vs. 51 h). In this case, the reaction was performed using 2.2 equivalents of ICl in dichloromethane at reflux. Single crystals suitable for X-ray structural determination were obtained by slow diffusion of cyclohexane into a DCM solution of **2b**. As illustrated in Figure 3, the structure confirms the molecular integrity of the compound. The iodo-benzophosphole fragment is essentially coplanar (average

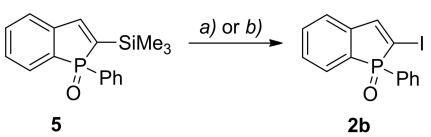

Scheme 2. Iododesilylation of **5** to obtain iodide **2b**. *a)* NIS (3 equiv), CH_3CN, 35 °C, 17%; *b)* ICl (2.2 equiv), DCM, reflux, 80%.

Research Article
doi.org/10.1002/ejoc.202201209

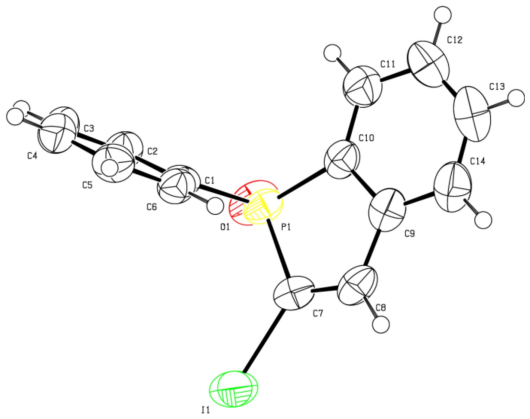

Figure 3. ORTEP view of benzo[*b*]phosphole halide **2b**.

deviation from the least squares plane (lsp) 0.017 Å). The bond metrics are unexceptional with endocyclic P–C distances of 1.807(6) and 1.799(6) Å, and an exocyclic P–C_{Ph} distance of 1.796(6). The sum of the C–P–C angles is 308.5° illustrating the pyramidalization at the phosphine oxide center. The PO bond (1.482(4) Å) encompasses a 38.4° angle with the aforementioned lsp, imparting a large dipole moment to this motif.

Pathway A: Synthesis of (*E*)-1 through Heck reaction

According to Pathway A (Scheme 1), the synthesis of (*E*)-**1** through the Heck reaction between iodide **2b** and alkene **3** was attempted using experimental conditions very similar to those reported in Matano's work.[13b] As illustrated in Scheme 3, the reaction was carried out using a catalytic amount of $Pd(OAc)_2$ (4 mol%) in DMF at 120 °C for 24 h, and the required bis-(benzo[*b*]phosphole) *P*-oxide (*E*)-**1** was obtained as a mixture of *cis*-(*E*)-**1** and *trans*-(*E*)-**1** diastereoisomers (overall yield 19%).

The two diastereoisomers could be separated by column chromatography on silica gel. *cis*-(*E*)-**1** eluted first ($R_f = 0.38$, dichloromethane/acetone, 7:1) and was isolated in 11% yield, while the *trans*-(*E*)-**1** with a lower R_f of 0.22 (dichloromethane/acetone, 4:1) was isolated in 8% yield.

Pathway B: Homo-metathesis reaction of 2-vinyl-benzo[b]phosphole *P*-oxide 3

The metathesis reaction involving benzo[*b*]phosphole chalcogenides is quite an unexplored process,[18] and the homo-metathesis of **3** was explored according to a protocol reported for the olefin metathesis of vinyl and allyl diphenyl phosphine oxides.[19] Thus, a solution of **3** and the Grubbs' catalyst **6** was refluxed in CH_2Cl_2 for 43 h. After chromatographic purification of the crude mixture, *cis*-(*E*)-**1** and *trans*-(*E*)-**1** were isolated in 19% and 12% yield, respectively (Scheme 4).

Aiming to improve the reaction outcome, a brief screening of some experimental parameters (e.g., temperature and solvent) was carried out. However, the use of toluene instead of CH_2Cl_2 (at 40 or 110 °C) or chloroform (at 80 °C) did not result in any significant improvement.

Pathway C: Double Stille coupling reaction

This approach involves the synthesis of the target olefin (*E*)-**1** through a "one-pot" double Stille cross-coupling reaction between halides **2** and the commercially available *trans*-1,2-bis(tributylstannyl)ethylene (**4**) (Scheme 5).

A mixture of $Pd_2(dba)_3$, $(2\text{-furyl})_3P$ and 1-methyl-2-pyrrolidinone (NMP) was stirred for 1 h at room temperature. To this mixture, bromide **2a** or iodide **2b** (2.1 equiv.), stannane **4** (1 equiv.), CuI and NMP were added. The resulting mixture was stirred at 17 °C for 4 h. Using bromide **2a**, the two diastereoisomers of (*E*)-**1** were isolated in 20% (*cis*) and 12% (*trans*) yield (overall yield 32%). Better results were obtained using iodide **2b**: in this case *cis*-(*E*)-**1** and *trans*-(*E*)-**1** were isolated in 31% and 15% yield, respectively (overall yield 46%).

Both diastereoisomers of (*E*)-**1** were fully characterized by NMR and HR-MS spectroscopy. Their NMR assignment was carried out using 1- and 2-dimensional experiments, to obtain the resonances of both ^1H and ^{13}C (reported in Table S2). To assign the resonances of the protons, NOESY experiment was used for the identification of the interaction between olefinic and benzophosphole protons (H1 and H3, see Table S2). In particular, similar resonances were observed for the benzophosphole protons in the two diastereoisomers, while a differ-

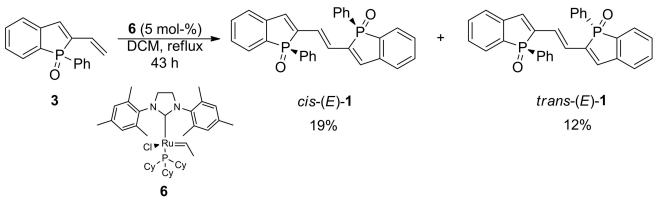

Scheme 4. Synthesis of *cis*-(*E*)-**1** and *trans*-(*E*)-**1** through homo-metathesis reaction of **3**.

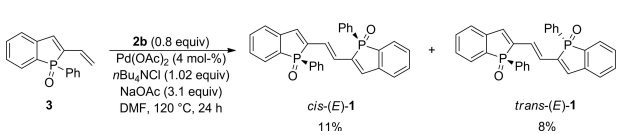

Scheme 3. Synthesis of *cis*-(*E*)-**1** and *trans*-(*E*)-**1** through Heck reaction.

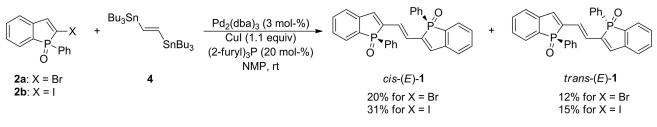

Scheme 5. Synthesis of *cis*-(*E*)-**1** and *trans*-(*E*)-**1** through double Stille coupling reaction.

Research Article
doi.org/10.1002/ejoc.202201209

ence in terms of ^{1}H chemical shift was observed for the phenyl ring bound to phosphorus.

In detail, ^{1}H NMR spectra acquired at 283 K exhibited, for the cis isomer, the chemical shift value of 7.75, 7.45 and 7.30 ppm for ortho, meta and para protons, respectively, while for the trans isomer, the same protons resonate at 7.63, 7.37 and 7.27 ppm (Table S2).

This difference can be ascribed to proton-proton steric interactions in the aromatic systems that can be observed for the *cis* isomer in which the two phenyl rings face each other's (see Figure 7), giving rise to deshielding effects on the proton chemical shifts.[27] This observation can be compared with the results observed in the CV experiments (see "electrochemical properties" paragraph) and allows the assignment of the configuration for the two molecules.

Also, the resonances of ^{31}P were identified as singlet peaks at 37.9 ppm and 38.3 for the two diastereoisomers, respectively.

According to literature reports the *cis*-diastereomer in related compounds show a shielded ^{31}P NMR signal compared to the *trans* diastereoisomer.[13c] Consequently, *cis*-(*E*)-**1** was assigned to the signal at 37.9 ppm, whereas *trans*-(*E*)-**1** showed a deshielded signal at 38.3 ppm. Therefore, also the chemical shift of ^{31}P can be used as indicator for *cis* or *trans* configuration.

Worth noting, the calculated ^{31}P NMR shifts obtained employing the GIAO formalism and described below in theoretical calculations section (−4.75 ppm for *cis*-(*E*)-**1** and −4.10 ppm for *trans*-(*E*)-**1**, see Supporting Information), beside the offset, perfectly agree with the observed experimental trend and thus supports this assignment.

Although no suitable crystals for X-ray analysis were obtained, we suggest the proper stereochemistry for the two diastereoisomers by combining NMR data, electrochemical behavior along with DFT calculations.

Furthermore, differential scanning calorimetry (DSC) analyses were performed under nitrogen atmosphere in a range of temperature starting from 25 °C to 350 °C, with a temperature rate of 10 °C/min (see Figures S9 and S10, Supporting Information). For *cis*-(*E*)-**1** we can observe three main points: 1) a possible enantiotropic transition related to a different metastable phase at 86.5 °C; 2) a sharp endothermic peak at 300.9 °C corresponding to the melting point; 3) a sharp exothermic peak at 303.7 °C corresponding to the instantaneous decomposition of the compound. These phenomena can also be confirmed by the black residue left on the sample after the heating cycle. For the *trans*-(*E*)-**1**, we observed a similar situation: a sharp endothermic peak at 268.1 °C corresponding to the melting point and a sharp exothermic peak at 281.9 °C corresponding to the instantaneous decomposition of the compound that leads to the formation of a black residue after the heating cycle. These data show that these compounds are stable up to 260–300 °C.

Optical studies

The optical properties of *cis*-(*E*)-**1** and *trans*-(*E*)-**1** were investigated by means of absorption spectroscopy which prove the two systems to be almost undistinguishable except for the lowest energy transitions around 420 nm. This absorption is slightly more intense in the *trans* compared to the *cis* isomer (Figure 4a). In CH_2Cl_2 solution at room temperature, the absorption spectra (Figure 4a) are characterized by two major transitions, one at high energy at 270 nm ($\varepsilon = 30000\ cm^{-1}M^{-1}$) and a second with a maximum at 395 nm ($\varepsilon = 39000\ cm^{-1}M^{-1}$). The resolved fine structure of the low energy band is typical of π-π^* transitions in rigid conjugated systems.

The *cis*-(*E*)-**1** was further characterized by emission spectroscopy both at room temperature and at 77 K in a frozen matrix of 2-MeTHF. Compound *cis*-(*E*)-**1** shows a broad and unstructured fluorescence with a maximum at 483 nm (Figure 4b). The emission quantum yield is 0.52 with a lifetime of 6.14 ns. The excitation spectrum perfectly matches the absorption one, confirming the absence of any aggregates and that the emission arises from the conjugated system of the molecule. Compound *cis*-(*E*)-**1** exhibits a higher emission efficiency with respect to the close related BPO compounds **A**[13c] and **B**[11f] (Figure 1). In addition, the overall redshift indicates a better conjugation when the two BPO units are connected through a carbon-carbon double bond with respect to a direct connection as in compound **A** or an aryl bridge as in compound **B**.

At 77 K, in rigid matrix of 2-MeTHF, the fluorescence spectrum features a more structured and vibrationally resolved shape (three clear peaks observable) with respect to the room temperature one (Figure 4c); the emission lifetime is 5.5 ns. The almost perfect mirror image of the low temperature emission

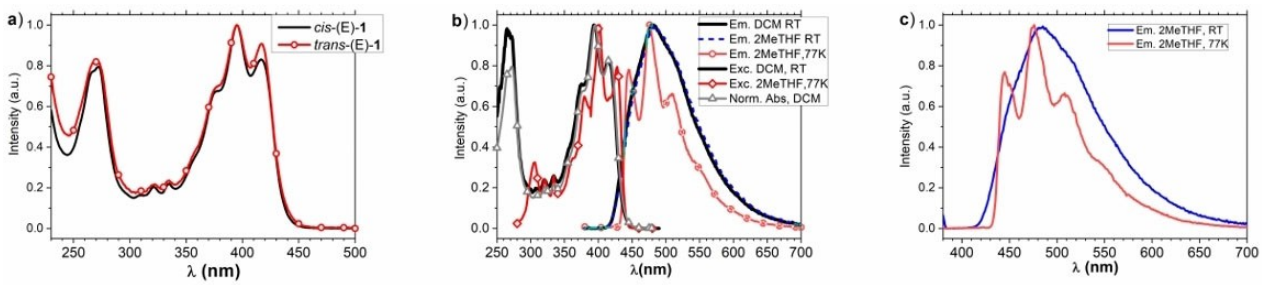

Figure 4. a) Absorption spectra in DCM solution of the *cis*-(*E*)-**1** and *trans*-(*E*)-**1**; b) emission and excitation spectra of *cis*-(*E*)-**1**; c) compared emissions at RT and 77 K.

Research Article
doi.org/10.1002/ejoc.202201209

spectrum and its corresponding absorption spectrum is indicative of an overall rigid structure in glassy matrix. Moreover, this behaviour indicates a significant geometrical distortion of the molecule in the excited state compared to that of the ground state. Hence, we can attribute the room temperature broad emission to rotovibrational modes and conformational freedom of the molecule in fluid solution.

Electrochemical properties

The electronic properties of *cis*-(*E*)-**1** and *trans*-(*E*)-**1** and those of precursors **2a** and **2b** were investigated by cyclic voltammetry (CV, Figure 5).

The first oxidation and the first reduction processes that are observed in the CVs provide information on the HOMO/LUMO levels for the four compounds and are summarized in Table 1.

From a previous work reported in literature,[20] the reduction of the phosphine oxide group is located at very negative potentials (~ −2.8 V vs. $Fc^{+/0}$). In this light, the first irreversible reduction peaks observed in the CVs of **2a** and **2b** at $E_{c,p}$ = −2.03 V and −1.98 V, respectively, are attributed to the cleavage of the C–X bond. The more cathodic redox features at −2.31 V and −2.33 V are assigned to the reduction of the aromatic systems of **2a** and **2b**, respectively (all potentials reported hereafter are vs. $Fc^{+/0}$).[21] Actually, the first two reduction peak system is typical of the aryl bromide family. In particular, shape and potentials of **2a** and **2b** peaks are very similar to those of *p*-Br-benzophenone, which, like in **2a** and **2b** case, is highly reactive.[21]

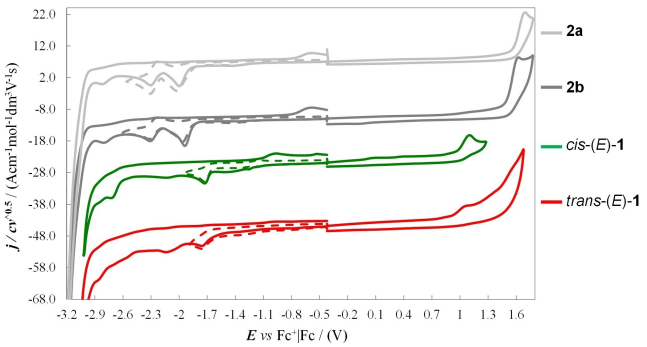

Figure 5. Normalized CVs on glassy carbon (GC) electrode at 200 mV/s potential scan rate in CH_3CN + 0.1 M $TBAPF_6$ as supporting electrolyte of **2a** (light grey), **2b** (dark grey), *cis*-(*E*)-**1** (green line) and *trans*-(*E*)-**1** (red line) (0.00075 M).

Table 1. HOMO and LUMO and relative energy gap values of the analysed compounds.

	$E_{p,Ia}$[a]/V	$E_{p,Ic}$[b]/V	E_{HOMO}[c]/eV	E_{LUMO}[d]/eV	H–L Gap/eV
2a	1.72	−2.03	−6.52	−2.77	3.75
2b	1.65	−1.98	−6.45	−2.82	3.63
cis-(*E*)-**1**	1.12	−1.76	−5.92	−3.04	2.88
trans-(*E*)-**1**	1.08	−1.77	−5.88	−3.03	2.85

[a] $E_{p,Ia}$ = first oxidation peak potential. [b] $E_{p,Ic}$ = first reduction peak potential. [c] E_{HOMO} (eV) = −1e × [($E_{p,Ia}$/V(Fc + | Fc) + 4.8 V(Fc^+ | Fc vs. zero)] (maxima criterion). [d] E_{LUMO} (eV) = −1e × [($E_{p,Ic}$/V(Fc^+ | Fc) + 4.8 V(Fc^+ | Fc vs. zero)] (maxima criterion).

Moreover, the CV pattern of precursors **2a** and **2b** (see also Supporting Information) is consistent with a stepwise dissociative electron transfer (DET) mechanism for the reductive cleavage of the C–X bond, consisting of a fast ET resulting in a stable radical anion, followed by cleavage of the C–X bond to give $R^•$ radical and X^- anion. This is suggested by the evaluation of the ET barrier symmetry coefficient α (0.77 for **2a** and 0.75 for **2b**), estimated by the following equation $\delta E_p/\delta \log v = -1.15RT/F\alpha$.[22–25]

Electrochemical reductive cleavage of C–X bonds can lead to either dehydrohalogenation or coupling/dimerization products. The former outcome is typical of aromatic halides, while the latter is predominantly observed in aliphatic and benzyl halides. In this respect, it would be interesting to perform semipreparative experiments with the present halogenated benzophospholes in the future.

In case of *cis-(E)*-**1** and *trans-(E)*-**1**, the first reductions are observed at $E_{c,p}$ = −1.76 and −1.77 V, respectively. The electron uptakes are probably related to the formation of the radical anion on the extended π-conjugated system, while the second reductions are associated to the phosphine oxide (−2.71 V and −2.83 V).[26]

Comparing the CVs of precursors and diastereoisomers (Figure 5), *cis-(E)*-**1** and *trans-(E)*-**1** are characterized by a more positive reduction peak and a more negative oxidation peak, which could be justified in terms of extended conjugation induced by the double bond between the two benzophosphole units. According to these observations, the two diastereoisomers have a narrower HOMO-LUMO gap (Table 1), due to the higher degree of π-conjugation. In particular, the reduction potentials of *cis-(E)*-**1** and *trans-(E)*-**1** can be observed at −1.76 and −1.77 V, that is, shifted by about 200–250 mV compared to those of the monomeric precursors; this trend is even more pronounced when comparing the oxidation potentials of *cis-(E)*-**1** and *trans-(E)*-**1** with those of **2a**,**b**, the oxidations in the former being observed at around 1.10 V, cathodically shifted by more than 500 mV compared to those of the latter.

Finally, a small but possibly significant difference is observed in the oxidation peak potential $E_{p,a}$ of *trans-(E)*-**1** *and cis-(E)*-**1**) at 1.08 V and 1.12 V, respectively. This is consistent with the two compounds being diastereoisomers and therefore electrochemically distinguishable.

Theoretical calculations

The geometries of the *trans* and *cis* (*E*)-**1** were optimized at the B3LYP/6-311g theory level to support the assignments of the different diastereoisomers. The method has been reported to provide confident results,[13c] and in our case parameters calculated for the benzo[*b*]phosphole *P*-oxide (BPO) core in **1** are consistent with crystallographic data of (±)-**2b**. TDDFT calculations have been performed to determine the lowest 10 excited states of the optimized geometry. In addition, the isotropic values of calculated absolute shielding constants for

^{31}P are computed for the optimized structures in gas phase using the gage-independent atomic orbital (GIAO) method at the same theory level used for the geometry optimizations (see Supporting Information).

The optimized geometries of *trans* and *cis* isomers are reported in Figure 6.

Trans-(*E*)-**1**, i.e., the isomer where the phenyl rings bonded to the P atoms are directed above and below the plane described by the BPO-ethene system, is characterized by a completely flat conjugated system which includes the ethene double bond and the two BPO moieties. The BPO-ethene bond length is in the range of 1.45 Å and the ethene double bond result to be 1.35 Å; the P–C bond lengths in the two phosphole rings range between 1.83–1.85 Å and the P=O distance is in the range of 1.49 Å like the distances reported in the literature for similar compounds and those of **2b** (this paper). The *cis*-(*E*)-**1**, i.e. the isomer with the two phenyl rings bonded to the P atoms directed towards the same side of the BPO-ethene plane, displays a rather distorted geometry of the conjugated BPO-ethene-BPO skeleton resulting in a twisted arrangement of one BPO moieties with respect to the other one and describing a dihedral angle between their average planes approaching 40°; the torsion appear to be the result of a partial (attractive) interaction between the P–Ph residues although these do not eclipse each other. Beside this structural conformation all other bond lengths are in the range reported for the *trans*-(*E*)-**1**.

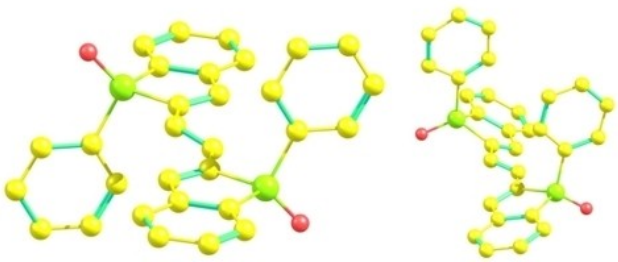

Figure 6. Optimized structures of the *trans*-(*E*)-**1** (left) and *cis*-(*E*)-**1** (right).

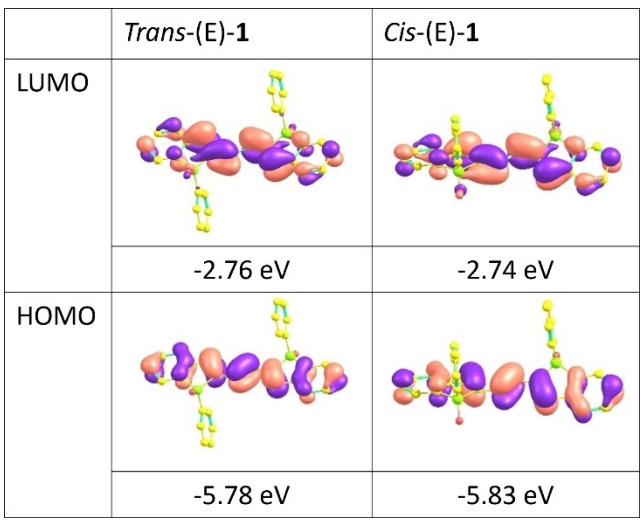

Figure 7. Frontier orbitals plot (HOMO and LUMO) and corresponding energies of the *trans*-(*E*)-**1** (left) and *cis*-(*E*)-**1** (right).

The calculated frontier molecular orbital energies and relative plots are reported in Figure 7 and Table S3 and Figure S15 (Supporting Information). Overall, in both diastereoisomers, the HOMO and LUMO spread over the two BPO units and the double bond. It is noteworthy that the small torsion angle between the BPO units and the double bond in *cis*-(*E*)-**1** does not preclude the conjugation to spread over the whole molecule. Apparently, no contribution comes from the P atoms in these orbitals. Interestingly, the energy values of the frontier levels are in quite good agreement with the corresponding values measured by cyclic voltammetry, within the typical 100 meV shift between experiment and theory (which do not account for solvent effects). For the HOMO values, it is interesting to observe that calculations seemingly reproduce the ca. 50 meV difference in HOMO energies with the *cis*-(*E*)-**1** value slightly more negative than that of the *trans*-(*E*)-**1**. In analogy to the experimental CV trends (Table 1), the result is suggesting that the compound with the deeper HOMO has a *cis* geometry, likewise the other has *trans* geometry.

In both compounds, the LUMOs lie close in energy, in line with the values obtained from the CV experiments (Table 1). Thus, the theoretical HOMO-LUMO gaps (being 2.92 and 2.99 eV for *trans* and *cis*, respectively) nicely reproduce the trend experimentally determined by CV (Table 1). TDDFT calculations indicate that the lowest energy absorption in *trans*-(*E*)-**1** (calc. 444 nm) and *cis*-(*E*)-**1** (calc. 437 nm) is associated with a HOMO-LUMO transition and consequently has π-π* characteristics.

Finally, employing the GIAO formalism, we calculated the ^{31}P NMR shift of *trans*-(*E*)-**1** (−4.10 ppm) and *cis*-(*E*)-**1** (−4.75 ppm) to compare the trend and the shifts gap with the experimental values inferred from NMR.

Conclusion

In summary, we have investigated three synthetic methodologies (A, B and C, Scheme 1) for the synthesis of a π-conjugated benzo[*b*]phosphole *P*-oxide in which two phosphole *P*-oxide units are connected by a carbon-carbon double bond. We have found that the double Stille approach (pathway C) was most efficient for the synthesis of the title compounds. Due to the presence of the two stereogenic phosphorus atoms, the bis-BPO-ethylene was isolated as a mixture of the two *cis* and *trans* diastereoisomers (the chiral and the meso one respectively) that could be separated by column chromatography and fully characterized. The electrochemical and photophysical behaviour of the isolated *cis* and *trans* isomers were investigated, and their frontier molecular orbital energies calculated. The calculated HOMO-LUMO gaps reproduced the trends from the CV experiments very well. The configuration of the two diastereoisomers has been assigned based on CV experiments as well as on chemical shifts of the protons of phenyl rings on the P atoms, which resulted to be deshielded in the *cis* isomer due to proton-proton steric interaction.

Experimental Section

General Information: All the reactions were carried out under inert atmosphere (nitrogen or argon) by means of standard Schlenk technique for manipulating air-sensitive compounds. Anhydrous DCM, DMF and NMP in 100 mL bottles containing molecular sieves and equipped with crown caps were used once required in the synthesis. Compounds **5**,[17] **2a**[13c] and **3**[13b] were synthesized following literature procedures. Reactions were monitored by thin-layer chromatography (TLC) using Aldrich silica gel 60 F254 precoated plates. Column chromatography was carried out with silica gel (70–230 mesh). Melting points were determined with a Büchi Melting Point B-540 apparatus and are uncorrected. NMR spectroscopy experiments were performed at 298 and 283 K on Bruker Avance 400 and 600 MHz spectrometers. The NMR experiments were carried out in $CDCl_3$ at a concentration of 10 mM. 1D-^{1}H, 1D-^{13}C and 1D-^{31}P spectra and two-dimensional homonuclear (^{1}H,^{1}H-COSY and ^{1}H,^{1}H-NOESY) and heteronuclear (^{1}H,^{13}C-HSQC and ^{1}H,^{13}C-HMBC with a long-range $J = 8$ Hz) experiments were acquired. For 1D-^{1}H, 30-degree flip angle sequence and inverse gated decoupling (for the decoupling with ^{31}P) are acquired and used for the assignment. For 1D-^{13}C, APT (attached proton) and ig (inverse gated decoupling) sequence are applied, with 15360 scans. For 1D-^{31}P, ig (inverse gated decoupling) sequence is used for the determination of phosphorus resonance (see Figure S8, Supporting Information). The assignment of compound **2b** is reported in Table S1 (Supporting Information). The complete NMR assignment for *cis*-(*E*)-**1** and *trans*-(*E*)-**1** is obtained for all resonances and is reported in Table S2 (Supporting Information). DSC analyses were recorded with a Mettler Toledo Star™ SW equipped with a HUBER TC100-MT RC 230 V COOLING SYSTEM. The IR spectra were recorded on powder samples using an ATR Fourier Transform Infrared (FTIR) spectrometer (PerkinElmer spectrum 100). High Resolution Electron Ionization (HR EI) mass spectra were recorded on a FISONS-Vg Autospec-M246 spectrometer.

Synthesis of iodide 2b: To a stirring solution of **5** (1.84 mmol, 0.55 g) in dry DCM (25 mL) at 0 °C, a solution of ICl (6 mL, 6.9 mmol, 1 M in DCM) was added dropwise under nitrogen atmosphere, and the resulting mixture was stirred at reflux. After 4 h, the reaction mixture was cooled to room temperature, a saturated aqueous solution of $Na_2S_2O_3$ (80 mL) was added, and the aqueous phase was extracted with DCM (4×20 mL). The collected organic phases were washed with water (2×20 mL), dried over Na_2SO_4, and concentrated under reduced pressure. The residue was purified by column chromatography on silica gel (DCM:acetone 10:1) to afford **2b** (521 mg, 80%) as a colourless solid, m.p. (hexane:DCM) 167–169 °C. IR (neat): $\tilde{\nu} = 3050$, 2922, 1995, 1717, 1589, 1530, 1455, 1440, 1306, 1289, 1236, 1196, 1179, 1167, 1130, 1112, 1070, 1023, 997, 958, 922, 904, 878, 756, 728, 696, 617, 605, 565, 535, 526, 507, 477, 439, 405 cm^{-1}. ^{31}P NMR ($CDCl_3$, 125 MHz) $\delta = +39.1$ ppm. HRMS (EI): calculated for $C_{14}H_{10}IOP$ $[M]^+$: 351.9503, found 351.9514. For the ^{1}H and ^{13}C NMR data, see Table S1, Supporting Information.

Synthesis of (*E*)-1 through Heck reaction (Pathway A): Iodide **2b** (85 mg, 0.24 mmol), olefin **3** (69 mg, 0.27 mmol), nBu$_4$NCl (65 mg, 0.25 mmol), NaOAc (61 mg, 0.75 mmol) and $Pd(OAc)_2$ (2.17 mg, 0.09 mmol) were dissolved in dry DMF (13 mL) under an argon atmosphere. The resulting mixture was stirred at 120 °C for 24 h, and a saturated NH_4Cl aqueous solution (50 mL) was then added to the mixture. The aqueous phase was extracted with DCM (4× 10 mL), and the collected organic phases were washed with water (2×20 mL), dried over Na_2SO_4, and concentrated under reduced pressure. The residue was purified by column chromatography on silica gel (DCM:acetone, 10:1 to 4:1) to provide the *cis*-(*E*)-**1** (13 mg, 11%) and *trans*-(*E*)-**1** (9 mg, 8%) as yellow solids (19% overall yield).

Synthesis of (*E*)-1 through homo-metathesis reaction (Pathway B): Olefin **3** (87 mg, 0.34 mmol) was dissolved in dry DCM (5 mL), and Grubbs' catalyst **6** (15 mg, 0.018 mmol) was added. The resulting mixture was stirred at reflux for 9 h under a nitrogen atmosphere. Afterwards, the mixture was cooled to room temperature, and the solvent was removed under reduced pressure. The residue was purified by column chromatography on silica gel (DCM:acetone, 10:1 to 4:1) to provide the *cis*-(*E*)-**1** (15 mg, 19%) and *trans*-(*E*)-**1** (10 mg, 12%) as yellow solids (31% overall yield).

Synthesis of (*E*)-1 through double Stille coupling (Pathway C): A mixture of $Pd_2(dba)_3$ (17 mg, 0.02 mmol), (2-furyl)$_3$P (28 mg, 0.12 mmol), and dry NMP (4 mL) was stirred for 1 h at room temperature under a nitrogen atmosphere. Next, iodide **2b** (427 mg, 1.12 mmol), stannane **4** (0.31 mL, 0.58 mmol), CuI (121 mg, 0.64 mmol) and NMP (16 mL) were added. The resulting mixture was stirred for 3.5 h at room temperature under a nitrogen atmosphere. The mixture was poured into a saturated NH_4Cl aqueous solution (100 mL). The aqueous phase was extracted with toluene (10×20 mL), the collected organic phases were washed with H_2O (3×100 mL), dried over Na_2SO_4, and concentrated under reduced pressure. The residue was purified by column chromatography on silica gel (DCM:acetone, 10:1 to 4:1) to provide the *cis*-(*E*)-**1** (83 mg, 31%) and *trans*-(*E*)-**1** (40 mg, 15%) as yellow solids (46% overall yield). Iodide **2b** was also recovered (81 mg).

***cis*-(*E*)-1**: m.p. (pentane) 300.9 °C. ^{31}P NMR ($CDCl_3$, 125 MHz) $\delta = +37.9$ ppm. IR (neat): $\tilde{\nu} = 3067$, 3008, 1588, 1547, 1482, 1447, 1435, 1308, 1283, 1232, 1192, 1171, 1128, 1109, 1065, 1028, 990, 941, 910, 855, 755, 745, 722, 707, 691, 672, 619, 592, 530, 503, 471, 449, 430 cm^{-1}. HRMS (EI): calcd for $C_{30}H_{22}O_2P_2$ $[M]^+$: 476.1095, found 476.1091. For the ^{1}H and ^{13}C NMR data, see Table S2, Supporting Information.

***trans*-(*E*)-1**: m.p. (pentane) 268.1 °C. ^{31}P NMR ($CDCl_3$, 125 MHz) $\delta = +38.3$ ppm. IR (neat): $\tilde{\nu} = 3452$, 3012, 1589, 1549, 1483, 1451, 1439, 1305, 1275, 1185, 1128, 1109, 1065, 1027, 978, 913, 859, 847, 757, 747, 738, 722, 705, 687, 671, 615, 592, 550, 537, 527, 511, 495, 486, 463, 452 cm^{-1}. HRMS (EI): calcd for $C_{30}H_{22}O_2P_2$ $[M]^+$: 476.1095, found 476.1079. For the ^{1}H and ^{13}C NMR data, see Table S2, Supporting Information.

Deposition Number 2205296 (for **2b**) contains the supplementary crystallographic data for this paper. These data are provided free of charge by the joint Cambridge Crystallographic Data Centre and Fachinformationszentrum Karlsruhe Access Structures service.

Optics: The absolute photoluminescence quantum yields were measured with a spectrofluorimeter Hamamatsu QY-C11347 Quantaurus provided with a 150 W Xenon lamp, integration sphere and a multichannel analyzer. UV/Vis absorption spectra were obtained on Shimadzu UV-Vis-NIR 3600 Spectrophotometer in 1 cm path length quartz cell. Steady state emission and excitation spectra were recorded with a FLS 980 (Edinburgh Instrument Ltd.) equipped with a 450 W Xenon arc lamp. The photoluminescence lifetime measurements were determined via TCSPC (time correlated single photon counting) routine, using a pulsed LED source and a laser one form Edinburgh (Edinburgh Instrument Ltd.). The photoluminescence experiment at room temperature were performed in air saturated DCM solutions and 2-MeTHF one in concentration of 2×10^{-5} M. Low temperature experiments were run in 2-MeTHF solution at 77 K.

Electrochemistry: The electrochemical experiments were carried out using an AutoLab PGStat potentiostat and a classical three-electrode glass minicell (working volume about 3 mL), including as working electrode a glassy carbon GC disk (Metrohm, S = 0.033 cm^2) polished by diamond powder (1 μm Aldrich) on a wet cloth (Struers DP-NAP), as counter electrode a platinum disk, and as reference

electrode a saturated aqueous calomel one (SCE) inserted in a compartment with the working medium ending in a porous frit, to avoid contamination of the working solution by water and KCl traces. Experiments were run at scan rates ranging 0.05–2 V/s on 0.00075 M solutions in $CH_3CN + 0.1$ M tetrabutylammonium hexafluorophosphate $TBAPF_6$ as the supporting electrolyte, previously deaerated by nitrogen bubbling. Positive and negative half cycles have been separately recorded to avoid reciprocal contamination by electron transfer products. The reported potentials have been normalized vs. the formal potential of the intersolvental ferricinium/ferrocene ($Fc^+|Fc$) reference redox couple, recorded in the same conditions.

Acknowledgements

University of Milan for V.P. PhD fellowship. This study was supported by Regione Lombardia and Fondazione CARIPLO (grant numbers 12689/13, 7959/13; Azione 1 e 2, "SmartMatLab centre"), the Italian MUR under the project PRIN 2017 (grant no. 2017FJCPEX "3DFARE: Functional 3D architectures for electrochemiluminescence applications"), and the Swedish Research Council (grant nr. 2015-04640). The authors thank Fondazione "Banca del Monte di Lombardia" for the funding of the LCMS2020 mass spectrometer, and the Swedish Research Council (grant nrs. 2015-04640 (SO) and 2017-03727_(AO)).

Conflict of Interest

The authors declare no conflict of interest.

Data Availability Statement

The data that support the findings of this study are available from the corresponding author upon reasonable request.

Keywords: benzophospholes · cyclic voltammetry · diastereomers · fluorescence · π-conjugation

[1] a) M. P. Duffy, W. Delaunay, P. A. Bouit, M. Hissler, *Chem. Soc. Rev.* **2016**, *45*, 5296–5310; b) C. Reus, T. Baumgartner, *Dalton Trans.* **2016**, *45*, 1850–1855; c) M. A. Shameem, A. Orthaber, *Chem. Eur. J.* **2016**, *22*, 10718–10735; d) Y. Matano, *Chem. Rec.* **2015**, *15*, 636–650; e) T. Baumgartner, *Acc. Chem. Res.* **2014**, *47*, 1613–1622; f) Y. Ren, T. Baumgartner, *Dalton Trans.* **2012**, *41*, 7792–7800; g) Y. Matano, H. Imahori, *Org. Biomol. Chem.* **2009**, *7*, 1258–1271; h) J. Crassous, R. Réau, *Dalton Trans.* **2008**, *48*, 6865–6876; i) M. Hissler, C. Lescop, R. Réau, *Pure Appl. Chem.* **2007**, *79*, 201–212; j) T. Baumgartner, R. Réau, *Chem. Rev.* **2006**, *106*, 4681–4727.

[2] L. Nyulászi, *Chem. Rev.* **2001**, *101*, 1229–1246.

[3] a) N. M.-W. Wu, M. Ng, V. W.-W. Yam, *Angew. Chem. Int. Ed.* **2019**, *58*, 3027–3031; *Angew. Chem.* **2019**, *131*, 3059–3063; b) M. Matsumura, M. Yamada, A. Muranaka, M. Kanai, N. Kakusawa, D. Hashizume, M. Uchiyama, S. Yasuike, *Beilstein J. Org. Chem.* **2017**, *13*, 2304–2309.

[4] a) A. S. Nenashev, D. A. Dospekhov, T. A. Podrugina, *Mendeleev Commun.* **2021**, *31*, 618–619; b) Y. Koyanagi, S. Kawaguchi, K. Fujii, Y. Kimura, T. Sasamori, N. Tokitoh, Y. Matano, *Dalton Trans.* **2017**, *46*, 9517–9527; c) S. Arndt, M. M. Hansmann, P. Motloch, M. Rudolph, F. Rominger, A. S. K. Hashmi, *Chem. Eur. J.* **2017**, *23*, 2542–2547; d) A. Fukazawa, H. Yamada, Y. Sasaki, S. Akiyama, S. Yamaguchi, *Chem. Asian J.* **2010**, *5*, 466–469; e) A. Fukazawa, H. Yamada, S. Yamaguchi, *Angew. Chem. Int. Ed.* **2008**, *47*, 5582–5585; *Angew. Chem.* **2008**, *120*, 5664–5667.

[5] B. Wu, M. Santra, N. Yoshikai, *Angew. Chem. Int. Ed.* **2014**, *53*, 7543–7546; *Angew. Chem.* **2014**, *126*, 7673–7676.

[6] M. Kumaravel, J. T. Mague, M. S. Balakrishna, *Tetrahedron Lett.* **2014**, *55*, 2957–2961.

[7] a) Z. Zhuang, F. Bu, W. Luo, H. Peng, S. Chen, R. Hu, A. Qin, Z. Zhao, B. Z. Tang, *J. Mater. Chem. C* **2017**, *5*, 1836–1842; b) Y. Zhou, S. Yang, J. Li, G. He, Z. Duan, F. Mathey, *Dalton Trans.* **2016**, *45*, 18308–18312.

[8] H. Tsuji, K. Sato, Y. Sato, E. Nakamura, *Chem. Asian J.* **2010**, *5*, 1294–1297.

[9] a) S. M. Parke, S. Tanaka, H. Yu, E. Hupf, M. J. Ferguson, Y. Zhou, K. Naka, E. Rivard, *Macromolecules* **2019**, *52*, 7477–7488; b) C. Wang, A. Fukazawa, Y. Tanabe, N. Inai, D. Yokogawa, S. Yamaguchi, *Chem. Asian J.* **2018**, *13*, 1616–1624; c) R. A. Adler, C. Wang, A. Fukazawa, S. Yamaguchi, *Inorg. Chem.* **2017**, *56*, 8718–8725; d) C. Wang, M. Taki, Y. Sato, A. Fukazawa, T. Higashiyama, S. Yamaguchi, *J. Am. Chem. Soc.* **2017**, *139*, 10374–10381; e) C. Wang, A. Fukazawa, M. Taki, Y. Sato, T. Higashiyama, S. Yamaguchi, *Angew. Chem. Int. Ed.* **2015**, *54*, 15213–15217; *Angew. Chem.* **2015**, *127*, 15428–15432; f) E. Yamaguchi, C. Wang, A. Fukazawa, M. Taki, Y. Sato, T. Sasaki, M. Ueda, N. Sasaki, T. Higashiyama, S. Yamaguchi, *Angew. Chem. Int. Ed.* **2015**, *54*, 4539–4543; *Angew. Chem.* **2015**, *127*, 4622–4626; g) M. Taki, H. Ogasawara, H. Osaki, A. Fukazawa, Y. Sato, K. Ogasawara, T. Higashiyama, S. Yamaguchi, *Chem. Commun.* **2015**, *51*, 11880–11883; h) E. Yamaguchi, A. Fukazawa, Y. Kosaka, D. Yokogawa, S. Irle, S. Yamaguchi, *Bull. Chem. Soc. Jpn.* **2015**, *88*, 1545–1552; i) A. Fukazawa, Y. Ichihashi, Y. Kosaka, S. Yamaguchi, *Chem. Asian J.* **2009**, *4*, 1729–1740.

[10] a) S. Yamaguchi, A. Fukazawa, M. Taki, *J. Synth. Org. Chem. Jpn.* **2017**, *75*, 1179–1187; b) B. Wu, N. Yoshikai, *Org. Biomol. Chem.* **2016**, *14*, 5402–5416.

[11] a) B. Haruna, W. Hong, W. I. Mohamed, J. Guo, L. Ye, Y. Yin, Y. Gao, S. Tu, *J. Org. Chem.* **2021**, *86*, 13092–13099; b) J. Guo, C. Mao, B. Deng, L. Ye, Y. Yin, Y. Gao, S. Tu, *J. Org. Chem.* **2020**, *85*, 6359–6371; c) L. Liu, J. Dong, Y. Yan, S.-F. Yin, L.-B. Han, Y. Zhou, *Chem. Commun.* **2019**, *55*, 233–236; d) Y. Xu, Z. Wang, Z. Gan, Q. Xi, Z. Duan, F. Mathey, *Org. Lett.* **2015**, *17*, 1732–1734; e) Y. Zhou, Z. Gan, B. Su, J. Li, Z. Duan, F. Mathey, *Org. Lett.* **2015**, *17*, 5722–5724; f) T. Sanji, K. Shiraishi, T. Kashiwabara, M. Tanaka, *Org. Lett.* **2008**, *10*, 2689–2692; g) H. Tsuji, K. Sato, L. Ilies, Y. Itoh, Y. Sato, E. Nakamura, *Org. Lett.* **2008**, *10*, 2263–2265; h) A. Fukazawa, M. Hara, T. Okamoto, E.-C. Son, C. Xu, K. Tamao, S. Yamaguchi, *Org. Lett.* **2008**, *10*, 913–916.

[12] a) Á. Tajti, B. D. Kovács, N. Popovics-Tóth, F. Perdih, E. Bálint, *Tetrahedron* **2021**, *102*, 132527; b) W.-Q. Liu, T. Lei, S. Zhou, X.-L. Yang, J. Li, B. Chen, J. Sivaguru, C.-H. Tung, L.-Z. Wu, *J. Am. Chem. Soc.* **2019**, *141*, 13941–13947; c) V. V. Khrizanforova, K. V. Kholin, M. N. Khrizanforov, M. K. Kadirov, Y. H. Budnikova, *New J. Chem.* **2018**, *42*, 930–935; d) K. Nishimura, Y. Unoh, K. Hirano, M. Miura, *Chem. Eur. J.* **2018**, *24*, 13089–13092; e) D. Ma, W. Chen, G. Hu, Y. Zhang, Y. Gao, Y. Yin, Y. Zhao, *Green Chem.* **2016**, *18*, 3522–3526; f) V. Quint, F. Morlet-Savary, J.-F. Lohier, J. Lalevée, A.-C. Gaumont, S. Lakhdar, *J. Am. Chem. Soc.* **2016**, *138*, 7436–7441; g) P. Zhang, Y. Gao, L. Zhang, Z. Li, Y. Liu, G. Tang, Y. Zhao, *Adv. Synth. Catal.* **2016**, *358*, 138–142; h) G. Hu, Y. Zhang, J. Su, Z. Li, Y. Gao, Y. Zhao, *Org. Biomol. Chem.* **2015**, *13*, 8221–8231; i) W. Ma, L. Ackermann, *Synthesis* **2014**, *46*, 2297–2304; j) Y.-R. Chen, W.-L. Duan, *J. Am. Chem. Soc.* **2013**, *135*, 16754–16757; k) Y. Unoh, K. Hirano, T. Satoh, M. Miura, *Angew. Chem. Int. Ed.* **2013**, *52*, 12975–12979; *Angew. Chem.* **2013**, *125*, 13213–13217; l) T. Liu, X. Sun, L. Wu, *Adv. Synth. Catal.* **2018**, *360*, 2005–2012.

[13] a) Y. Matano, Y. Motegi, S. Kawatsu, Y. Kimura, *J. Org. Chem.* **2015**, *80*, 5944–5950; b) Y. Matano, Y. Hayashi, K. Suda, Y. Kimura, H. Imahori, *Org. Lett.* **2013**, *15*, 4458–4461; c) Y. Hayashi, Y. Matano, K. Suda, Y. Kimura, Y. Nakao, H. Imahori, *Chem. Eur. J.* **2012**, *18*, 15972–15983.

[14] A. Fukazawa, H. Osaki, S. Yamaguchi, *Asian J. Org. Chem.* **2014**, *3*, 122–127.

[15] a) E. Oberg, A. Örthaber, C. Lescop, R. Réau, M. Hissler, S. Ott, *Chem. Eur. J.* **2014**, *20*, 8421–8432; b) A. Kreienbrink, M. B. Sárosi, R. Kuhnert, P. Wonneberger, A. I. Arkhypchuk, P. Lönnecke, S. Ott, E. Hey-Hawkins, *Chem. Commun.* **2015**, *51*, 836–838; c) A. I. Arkhypchuk, M.-P. Santoni, S. Ott, *Angew. Chem. Int. Ed.* **2012**, *51*, 7776–7780; *Angew. Chem.* **2012**, *124*, 7896–7900.

[16] S. Xu, K. Nishimura, K. Saito, K. Hirano, M. Miura, *Chem. Sci.* **2022**, *13*, 10950–10960.

[17] J. Kurita, M. Ishii, S. Yasuike, T. Tsuchiya, *Chem. Pharm. Bull.* **1994**, *42*, 1437–1441.
[18] A. Tsurusaki, H. Matsumoto, K. Kamikawa, *Chem. Commun.* **2019**, *55*, 4909–4912.
[19] F. Bisaro, V. Gouverneur, *Tetrahedron Lett.* **2003**, *44*, 7133–7135.
[20] T. Benincori, V. Bonometti, R. Cirilli, P. R. Mussini, A. Marchesi, M. Pierini, T. Pilati, S. Rizzo, F. Sannicolò, *Chem. Eur. J.* **2013**, *19*, 165–181.
[21] A. A. Isse, P. R. Mussini, A. Gennaro, *J. Phys. Chem. C* **2009**, *113*, 14983–14992.
[22] J.-M. Savéant, *Elements of Molecular and Biomolecular Electrochemistry*, Wiley-Interscience: New York **2006**.
[23] J.-M. Savéant, *Adv. Phys. Org. Chem.* **2000**, *35*, 117–192.
[24] J.-M. Savéant, *Advances in Electron Transfer Chemistry*, P. S. Mariano, Ed.; JAI Press: New York **1994**, Vol. 4, pp. 53–116.
[25] R. S. Nicholson, I. Shain, *Anal. Chem.* **1964**, *36*, 706–723.
[26] E. Öberg, A. Orthaber, C. Lescop, R. Réau, M. Hissler, S. Ott, *Chem. Eur. J.* **2014**, *20*, 8421–8432.
[27] R. J. Abraham, M. Canton, M. Reid, L. Griffiths, *J. Chem. Soc. Perkin Trans. 2* **2000**, *4*, 803–812.

Manuscript received: October 17, 2022
Revised manuscript received: December 1, 2022